



المملكة العربية السعودية  
مدينة الملك عبدالعزيز للعلوم والتقنية  
الإدارة العامة لبرامج المنح البحثية

**المشروع البحثي التطبيقي أت -23- 40**

**التراكيب القشرية والوشاح العلوي تحت  
الدرع العربي والبحر الأحمر**

**التقرير النهائي المنقح**

**أ.د. عبدالله بن محمد العمري ( الباحث الرئيسي )  
أ.د. طارق بن علي الخليفة ( الباحث المشارك )**

**جامعة الملك سعود**

**ربيع الثاني 1428 هـ - مايو 2007 م**



**Kingdom of Saudi Arabia  
King Abdulaziz City for Science and Technology  
General Directorate of Research Grants Programs**

**AR – 23 – 40**

**REVISED FINAL REPORT**

**CRUSTAL AND UPPER MANTLE STRUCTURES BENEATH  
THE ARABIAN SHIELD AND RED SEA**

**Dr. Abdullah M. Al-Amri, KSU (P-I)  
Dr. Tariq A. Alkhalifah, KACST (CO-I)**

**KING SAUD UNIVERSITY**

**RABI II 1428 – MAY 2007**

جميع حقوق الطبع محفوظة لمدينة الملك عبدالعزيز للعلوم والتقنية. غير مسموح بطبع أي جزء من أجزاء هذا التقرير أو تخزينه في أي نظام تخزين المعلومات وإسترجاعها أو نقله على أي هيئة أو بأي وسيلة سواء كانت إلكترونية أو ممغنطة أو ميكانيكية، أو إستنساخاً، أو تسجيلاً، أو غيرها إلا بإذن من صاحب الطبع. إن كافة الآراء والنتائج والإستنتاجات والتوصيات المذكورة في هذا التقرير هي خاصة بالباحثين ولا تعكس وجهة نظر المدينة.

**All Rights Are Reserved to King Abdulaziz City for Science and Technology. No Part of this publication may be reproduced, stored in a retrieval system or transmitted in any form or by any means-electronic, electrostatic magnetic tape, mechanical, photocopying, recording or otherwise - without the permission of the copyright holders in writing. All views, results, conclusions, and recommendations in this report represent the opinions of the authors and do not reflect opinions of KACST.**

## **ACKNOWLEDGMENTS**

This is the final report of the research project **AR-23-40**. The authors would like to express their thanks and gratitude to King Abdulaziz City for Science and Technology for funding this project.

This work would not have been possible without the generous assistance of **KACST** and **KSU**.

Dr. Arthur Rodgers and Andrew Nyblade, the project consultants, whose expert guidance and continuing advice made this work possible. Their willingness to devote their time greatly facilitated the completion of the project. We owe them a deep debt of gratitude and a great deal of thanks.

Finally and most importantly, we would like to extend our sincerest thanks to Dr. Samantha Hansen, Hrvohe Tkalčić, Yongchoel Park and Mohammed Fnais who performed tomographic images and receiver functions and to Moustafa Hamed from KACST and Ahmed R. Khalil from KSU for collecting earthquake data.

## الخلاصة

يشتمل التقرير النهائي المنقح من المشروع البحثي التطبيقي أت-23-40 على نتائج التقارير الدورية الثلاثة السابقة بالإضافة إلى نتائج المرحلة النهائية من هذه الدراسة. تعتبر منطقة الدرع العربي والبحر الأحمر من الأماكن القليلة في العالم التي خضعت لشد قاري نشط وتكون قشرة بحرية حديثة. وعلى الرغم من قلة النشاط الزلزالي في معظم مناطق المملكة وخاصة الدرع العربي والمسطح العربي إلا أن قربها من المناطق النشطة زلزالياً في إيران وتركيا من ناحية الشمال الشرقي والبحر الأحمر والدرع العربي من جهة الغرب والجنوب الغربي وصدع البحر الميت التحولي شمالاً يتطلب دراسة التراكيب القشرية تحت الدرع العربي والبحر الأحمر للاستفادة منها في تحديد مواقع الزلازل بدقة عالية وتحديد مناطق الخطر الزلزالي المحتمل .

تهدف هذه الدراسة إلى تحديد تراكيب السرعة السيزمية للقشرة والجزء العلوي من الوشاح تحت هذه المنطقة باستخدام المعلومات الزلزالية واسعة المدى والمسجلة على شبكة الرصد الزلزالي التابعة لمدينة الملك عبدالعزيز للعلوم والتقنية. تشتمل الشبكة على 37 محطة زلزالية معظمها يتركز في الدرع العربي معطية نموذج ممتاز لدراسة الدرع العربي والبحر الأحمر. وتتميز محطات هذه الشبكة بقدرتها العاليه على إتقاط الإشارات الزلزاليه المحليه والاقليميه وهذا يعود إلى هدوء مواقع المحطات الحقلية.

قامت هذه الدراسة بإجراء تقنيات زلزالية حديثة على معلومات الشبكة ومن هذه التقنيات التي تم إجراؤها النمذجة الثلاثية البعد **Tomography** للمسارات الموجية الطولية و القصيرة للزلازل البعيدة المدى باستخدام طريقة المضاهاة المتقاطعة متعددة القنوات **MCCC** والتي أعطت صورة واضحة **image** للسرع الطولية والقصيرة للجزء العلوي من الوشاح والمرتبطة بالتغيرات الحرارية. أما النمذجة الثلاثية البعد للموجات الإقليمية المنكسرة من الموهو  $P_n$  فقد أستفيد منها في رسم تراكيب الموجات التضاغطية للوشاح الضحل. تمت نمذجة الموجات الطولية البعيدة المدى بواسطة دالة المستقبل **Receiver Functions** لتقدير عدم التوافق بين القشرة والجزء العلوي من الوشاح. تم تقدير دالة المستقبل من بيانات الشكل الموجي العالية الدقة من السجلات الزلزالية واسعة المدى ثلاثية الأبعاد والتي بلغ قدرها الزلزالي أكبر من 5.8 والمسافة الزلزالية ما بين 30 و90 درجة.

تم في هذه الدراسة استخدام الطرق متعددة المراحل **MSA4** وذلك لنمذجة منحنيات تشتت السرع الجماعية السطحية ( من 7 إلى 100 ثانية لموجات ريلي ومن 20 إلى 70 ثانية لموجات لوف) مع دوال المستقبل لتحديد تراكيب سرع الغلاف الصخري. تتكون الطريقة من أربع مراحل وتعتمد هذه الطريقة على بحث شبكي أولي لتركيب قشري بسيط وبعد ذلك تستخدم الطرق العكسية وبحث شبكي اخر لسرع موجات القص في الوشاح وأخيرا تم تطبيق النمذجة

التقدمية لتحليل الاختلاف في تشتت الموجات السطحية. وحيث أن الطرق العكسية لدوال المستقبل لها حساسية ضعيفة للسرع المضبوطة وللتغلب على هذه المشكلة فقد تم دمج سرع الموجات الجماعية في دوال المستقبل في شكل عكسي مع سرع القشرة والوشاح العلوي. أعطت نماذج السرع الزلزالية في هذه الدراسة تحفظات جديدة على تراكيب القشرة والوشاح العلوي لشبه الجزيرة العربية وحيث أن سماكة القشرة وسرعتها في هذه الدراسة متشابهة مع الدراسات السابقة إلا أن نتائج تراكيب الوشاح وخواصه السيزمية يعتبر جديد تماما ولم يسبق إجراؤه في المنطقة.

وأخيرا تم فصل موجات القص للزلازل بعيدة المدى لتقدير خواص الوشاح العلوي . دلت التحليلات على أن محطات منطقة خليج العقبة تشكل إتجاهات سريعة موازية لصدع البحر الميت التحويلي ومرتبطة مع الحركة المضربية بين أفريقيا وشبه الجزيرة العربية . بينما أعطت بقية المحطات في الدرع العربي نتائج إحصائية متشابهة وتأخذ شكلا متطابقا بإتجاه سريع شمال-جنوب مع معدل أزمنة تأخير قدرها 1,4 ثانية . ودمج الإنسياب الذي يأخذ إتجاه شمال شرق والمرتبطة بحركة الصفيحة المضبوطة مع الإنسياب الذي يأخذ إتجاه شمال غرب والمرتبطة بمثلث عفار على إمتداد البحر الأحمر تم إستنتاج محصلة تأخذ إتجاه شمال - جنوب مشابهة لنتائج الفصل وتؤيد نماذج الشد النشط ومراحل الإنفصال القاري.

يتغير تمدد قاع البحر الأحمر من شماله إلى جنوبه حيث يزداد التمدد كلما اتجهنا جنوباً ليصل إلى 14 ملم في السنة. يتضح من قراءة المقاطع التركيبية أن عمق الموهو والحد الفاصل بين الغلافين الصخري والوهن LAB أضحل بالقرب من البحر الأحمر ويزداد عمقها باتجاه المسطح العربي. يصل عمق الحد الفاصل بين الغلافين الصخري والوهن LAB إلى 55 كم تقريباً بالقرب من ساحل البحر الأحمر وما بين 100-110 كم تحت الدرع العربي أما عند حدود الدرع والمسطح العربي وصل عمق الـ LAB إلى 160 كم. تؤيد هذه الدراسة مبدأ النموذج المتعدد والذي يقترح أن هناك مجريين ريشيين تحت الدرع العربي وأن المناطق منخفضة السرعة (مناطق ذات درجة الحرارة الأعلى) مرتبطة بالنشاطات البركانية والخواص الطبوغرافية على سطح الدرع العربي.

علاوة على ذلك تقترح نتائج هذه الدراسة وجود مرحلتين من الشد في البحر الأحمر حيث التمدد والتعرية بالانسياب في الغلاف الوهن مسؤولة عن التغيرات في عمق الـ LAB. دلت طبوغرافية الـ LAB على انسياب الغلاف الوهن تحت الدرع العربي والبحر الأحمر والتي تلعب دوراً في التغيرات الحرارية للبيئة التكتونية.

وأخيراً توصي هذه الدراسة بإجراء عدد من الأبحاث الزلزالية الدقيقة لتخفيف مستوى الخطر

الزلزالي في شبه الجزيرة العربية ومن هذه الدراسات على سبيل المثال لا الحصر ما يلي :

٧ تحديث شبكة الرصد الزلزالي في جامعة الملك سعود من بيانية إلى رقمية وربطها

بشبكة مدينة الملك عبدالعزيز للعلوم والتقنية وهيئة المساحة الجيولوجية وتوحيد

برامج التشغيل بينها وذلك لتسهيل تبادل المعلومات و تحديد المعاملات الزلزالية بدقة

عالية .

٧ إجراء تراكيب قشرية باستخدام معطيات الجاذبية الأرضية والمغناطيسية الجوية في

المناطق التي تفتقر إلى محطات رصد زلازل ومقارنة نتائج هذه التراكيب بما

التوصل إليه من الطرق السيزمية الإنكسارية والزلزالية .

٧ تركيب راصدات الحركات الأرضية القوية في المناطق النشطة زلزالياً لحساب

معدلات تعميم الحركة الأرضية للاستفادة منها في تحديد معاملات الخطر الزلزالي

وعمل خرائط التمنطق الزلزالي وتطوير كود البناء.

## ABSTRACT

This final report of the research project AR-23-40 culminates the study reported in the previous three reports to estimate crustal and upper mantle structure. While there have been many studies of this topic using a wide variety of techniques, many questions about the structure of the Arabian Peninsula remain unanswered.

While for the most parts of Saudi Arabia, particularly, Arabian Shield and Arabian Platform are aseismic, the area is ringed with regional seismic sources in the tectonically active areas of Iran and Turkey to the northeast, the Red Sea Rift bordering the Shield to the southwest, and the Dead Sea Transform fault zone to the north.

The Arabian Shield and Red Sea region is considered one of only a few places in the world undergoing active continental rifting and formation of new oceanic lithosphere. We aim to determine the seismic velocity structure of the crust and upper mantle beneath this region using broadband seismic waveform data recorded by KACST seismic network. The network is operated by King Abdulaziz City for Science and Technology (KACST), Saudi Arabia and has 37 stations on the Arabian Shield and provides excellent sampling Shield and the adjacent Red Sea.

We estimate teleseismic receiver functions from high-quality waveform data. A raw data for RF analysis consist of 3-component broadband velocity seismograms for earthquakes with magnitudes  $M_w > 5.8$  and epicentral distances between  $30^\circ$  and  $90^\circ$ . We performed several modern seismic analyses of KACST data. Teleseismic P- and S-wave travel time tomography provide an image of upper mantle compressional and shear velocities related to thermal variations. We present a multiple step procedure for jointly fitting surface wave group velocity dispersion curves (from 7 to 100 seconds for Rayleigh and 20 to 70 seconds for Love waves) and teleseismic receiver functions for lithospheric velocity structure. The method relies on an initial grid search for a simple crustal

structure, followed by a formal iterative inversion, an additional grid search for shear wave velocity in the mantle and finally forward modeling of transverse isotropy to resolve surface wave dispersion discrepancy.

Inversions of receiver functions have poor sensitivity to absolute velocities. To overcome this shortcoming we have applied the method of *Julia et al.* (2000) that combines surface wave group velocities with receiver functions in formal inversions for crustal and uppermost mantle velocities. The resulting velocity models provide new constraints on crustal and upper mantle structure in the Arabian Peninsula. While crustal thickness and average crustal velocities are consistent with many previous studies, the results for detailed mantle structure are completely new.

Finally, teleseismic shear-wave splitting was measured to estimate upper mantle anisotropy. These analyses indicate that stations near the Gulf of Aqabah display fast orientations that are aligned parallel to the Dead Sea Transform Fault, most likely related to the strike-slip motion between Africa and Arabia. The remaining stations across Saudi Arabia are statistically the same, showing a consistent pattern of north-south oriented fast directions with delay times averaging about 1.4 s. The uniform anisotropic signature across Saudi Arabia is best explained by a combination of plate and density driven flow in the asthenosphere. By combining the northeast oriented flow associated with absolute plate motion with the northwest oriented flow associated with the channelized Afar plume along the Red Sea, we obtain a north-south oriented resultant that matches our splitting observations and supports models of active rifting processes. This explains why the north-south orientation of the fast polarization direction is so pervasive across the vast Arabian Plate.

Seafloor spreading in the Red Sea is non-uniform, ranging from nearly 0 cm/yr in the north to about 2 cm/yr in the south. Given the configuration of stations, we focused our examination along profile AA', which extends from the southern Red Sea Rift axis inland to station HASS. This allowed us to examine the most extensively rifted portion of the lithosphere as well as the structure beneath both

the Arabian Shield and Platform. However, for comparison, we also examined the more northern profile BB', which extends from the northern rift axis across the Arabian Shield to station ARSS.

The Moho and LAB are shallowest near the Red Sea and become deeper towards the Arabian interior. Near the coast, the Moho is at a depth of about 22-25 km. Crustal thickening continues until an average Moho depth of about 35-40 km is reached beneath the interior Arabian Shield. The LAB near the coast is at a depth of about 55 km; however it also deepens beneath the Shield to attain a maximum depth of 100-110 km. These boundary depths are comparable to those at similar distances along profile AA'. At the Shield-Platform boundary, a step is observed in the lithospheric thickness where the LAB depth increases to about 160 km.

This study supports multi plume model which is that there are two, separated plumes beneath the Arabian Shield, and the lower velocity zones (higher temperature zones) are related with volcanic activities and topographic characteristics on the surface of the Arabian Shield. In addition, our results suggest a two-stage rifting history, where extension and erosion by flow in the underlying asthenosphere are responsible for variations in LAB depth. LAB topography guides asthenospheric flow beneath western Arabia and the Red Sea, demonstrating the important role lithospheric variations play in the thermal modification of tectonic environments.

In order to fully understand the detail geophysical, seismological and seismic hazard picture of the Arabian Peninsula, this study recommends an extensive research covering :

A. An expensive but potentially insightful line of research is to carry out a detailed seismic deep refraction and gravity profiles in the Arabian Platform and along the coast of the Gulf of Aqabah to obtain a precise bulk composition of crustal layers and improve velocity model.

B. Upgrading of the existing system at King Saud University from analog to digital broadband recordings is strongly recommended for getting better quality signals.

C. Linking of KACST and KSU seismic networks with the national seismographic network at the Saudi Geological Survey is of great importance for getting better and dense station coverage as well as in facilitating data exchanges.

D. Installation of strong motion accelerographs in various areas of the Arabian Shield to precisely estimate the attenuation characteristics of the region and to improve seismic hazard parameters.

E. Assessment of seismic hazard in seismically active zones by constructing a probabilistic ground-shaking hazard map. This map will provide an estimate of the level of ground shaking at all sites expected from earthquake sources throughout the region (both local and regional). The map integrates the seismicity, attenuation and sit response factors.

F. A comprehensive study of the geotechnical engineering aspects should be done to account for local site effects and soil amplification.

G. A comprehensive study of seismogenic and faulting sources is needed for seismic zonation and microzonation of the Arabian Peninsula.

## DISCUSSION & CONCLUSIONS

Teleseismic data recorded on broadband instruments from four different seismic arrays were used in this study. The largest array, KACST seismic network, includes 27 broadband stations distributed along the eastern edge of the Red Sea and across the Arabian Peninsula. KACST data from events occurring since 2000 were used. To supplement the KACST coverage, we also analyzed data recorded by the eight IRIS-PASSCAL Saudi Arabian Broadband Array stations, which operated from November 1995 to March 1997, data from two stations deployed in Jordan, which operated between 1998 and 2001, and data recorded by two stations in the UAE from 2003 and 2004

S-waves with high signal-to-noise ratios were selected from earthquakes with magnitudes larger than 5.7 in a distance range of  $60^\circ$  to  $85^\circ$ . Waveforms were first rotated from the N-E-Z to the R-T-Z coordinate system using the event's back-azimuth and were visually inspected to pick the S-wave onset. The three-component records were then cut to focus on the section of the waveform that is 100 s prior to the S-wave onset and 20 s after. To more clearly detect Sp conversions, the cut R-T-Z data must be further rotated around the incidence angle into the SH-SV-P coordinate system and deconvolved. This second rotation is critical because if an incorrect incidence angle is used, noise can be significantly enhanced and major converted phases may become undetectable. A subroutine was developed, based on the approach of Sodoudi (2005), which rotates the cut R-T-Z seismograms through a series of incidence angles, from  $0^\circ$  to  $90^\circ$  in  $3^\circ$  increments, to create a set of quasi-SV and quasi-P data. Each quasi-SV component is then deconvolved from the corresponding quasi-P component using Ligorria and Ammon's iterative time domain method, which creates a SRF. To make the SRFs directly comparable to PRFs, both the time axes and the amplitudes of the

SRFs must be reversed. Using this approach, 31 different SRFs, corresponding to the 31 different incidence angles examined, are created for each event at a given station.

To limit our examination to the true P, SV components and their corresponding receiver function, we found the incidence angle that minimizes the direct S-wave energy on the P-component. On the time-reversed receiver functions, the direct S arrival is at 0 s. Therefore, we are only interested in the receiver function whose mean amplitude is closest to zero at zero time. A second subroutine was developed to examine all the generated receiver functions for a given event and determine which record best meets this criteria. The P, SV components and the corresponding receiver function with the appropriate incidence angle are retained, and the remaining records are discarded.

Once receiver functions were generated for all events at an examined station, a move-out correction was applied to the receiver functions to correct for variations in distance between events. Again, to make the SRFs directly comparable to PRFs, we used a reference slowness of 6.4 s/deg. Each individual receiver function is then visually inspected and compared to previously determined PRFs at the same station to identify the Moho phase. Only SRFs that display a clear Moho conversion at the appropriate time are used for further analysis. These records were then stacked to obtain a better signal-to-noise ratio for the weaker LAB phase (Lithosphere / Asthenosphere Boundary).

It should be noted that a similar approach to that outlined above was also used to examine SKS arrivals. In this case, we examined earthquakes with magnitudes larger than 5.6 in a distance range from 85° to 120°. However, it was discovered that the SKS arrivals do not generate clear Sp conversions given their steeper angles of incidence. Therefore, further examination of SKS receiver functions was not pursued.

Synthetic receiver functions were generated using the reflectivity method to match the amplitude and timing of both the Moho and LAB conversions on the stacked SRFs. Using the programs “icmod” and “respknt”, the responses of an incoming S-wave to different three-layer velocity models were generated. These synthetic responses were then processed using the same approach outlined previously to obtain the synthetic SRFs. The amplitude and timing of the phases on the real and synthetic receiver functions were matched by adjusting the crustal, upper mantle, and lower mantle velocities as well as the depth of the Moho and the LAB. While these values varied from station to station, the average crustal and upper mantle S-wave velocities needed to fit the Moho amplitude were about 3.6 and 4.5 km/s, respectively. These are similar to the S-wave velocities used to fit the Moho amplitude on the SANDSN PRFs. To fit the LAB amplitude, an average lower mantle velocity of about 4.2 km/s is required. In all cases, a default Poisson’s ratio of 0.25 was used .

It should be noted that the average shear velocities and default Poisson’s ratio used to generate the synthetics differ from those found by waveform modeling. Rodgers et al.(1999) reported average crustal S-wave velocities of 3.7 and 3.5 km/s and average upper mantle S velocities of 4.3 and 4.55 km/s for the Arabian Shield and Platform, respectively. In addition, the reported Poisson’s ratio in the Arabian Shield mantle was 0.29 while in the Platform it was 0.27. Testing revealed that the waveform modeling velocities did not fit the SRF phase amplitudes as well, but the timing of the phases only changed by a few tenths of a second. Therefore, the difference in shear velocities only leads to a few kilometers difference in depth. However, the timing of the phase conversions is more dependent on the Poisson’s ratio. Larger Poisson’s ratios, such as those suggested by the waveform modeling, result in earlier arrivals and hence shallower depths. Several tests were performed to examine how much the Moho and LAB depths changed when using the

Shield and Platform Poisson's ratio values. Based on the amount of variation observed, the reported Moho and LAB depths are accurate to within 5 and 10 km, respectively.

Seafloor spreading in the Red Sea is non-uniform, ranging from nearly 0 cm/yr in the north to about 2 cm/yr in the south. Given the configuration of stations, we focused our examination along profile AA', which extends from the southern Red Sea Rift axis inland to station HASS. This allowed us to examine the most extensively rifted portion of the lithosphere as well as the structure beneath both the Arabian Shield and Platform. However, for comparison, we also examined the more northern profile BB', which extends from the northern rift axis across the Arabian Shield to station ARSS.

Similar to profile AA', the Moho and LAB along BB' are shallowest near the Red Sea and become deeper towards the Arabian interior. Near the coast, the Moho is at a depth of about 22-25 km. Crustal thickening continues until an average Moho depth of about 35-40 km is reached beneath the interior Arabian Shield. The LAB near the coast is at a depth of about 55 km; however it also deepens beneath the Shield to attain a maximum depth of 100-110 km. These boundary depths are comparable to those at similar distances along profile AA' (Hansen et al., 2007).

The lithospheric structure along profile BB' was also tested by comparing its predicted gravity signature to data collected by the GRACE satellites. The same density values for the Arabian Shield used in the examination of profile AA' were employed. In addition, since profile BB' has fewer stations and therefore fewer constraints, we set the lithospheric thickness beneath the rift axis to be similar to that on profile AA' and examined if the calculated gravity signature is consistent with the recorded data. Small-scale recorded gravity observations can be matched very well by slightly adjusting the Moho and LAB boundaries (within the estimated error). Broad-scale gravity observations are also well fit by a shallow asthenosphere beneath the Red Sea. These results demonstrate that while seafloor spreading is not as developed in the northern Red Sea, the lithosphere has still been thinned and eroded by rifting processes (Hansen et al., 2007).

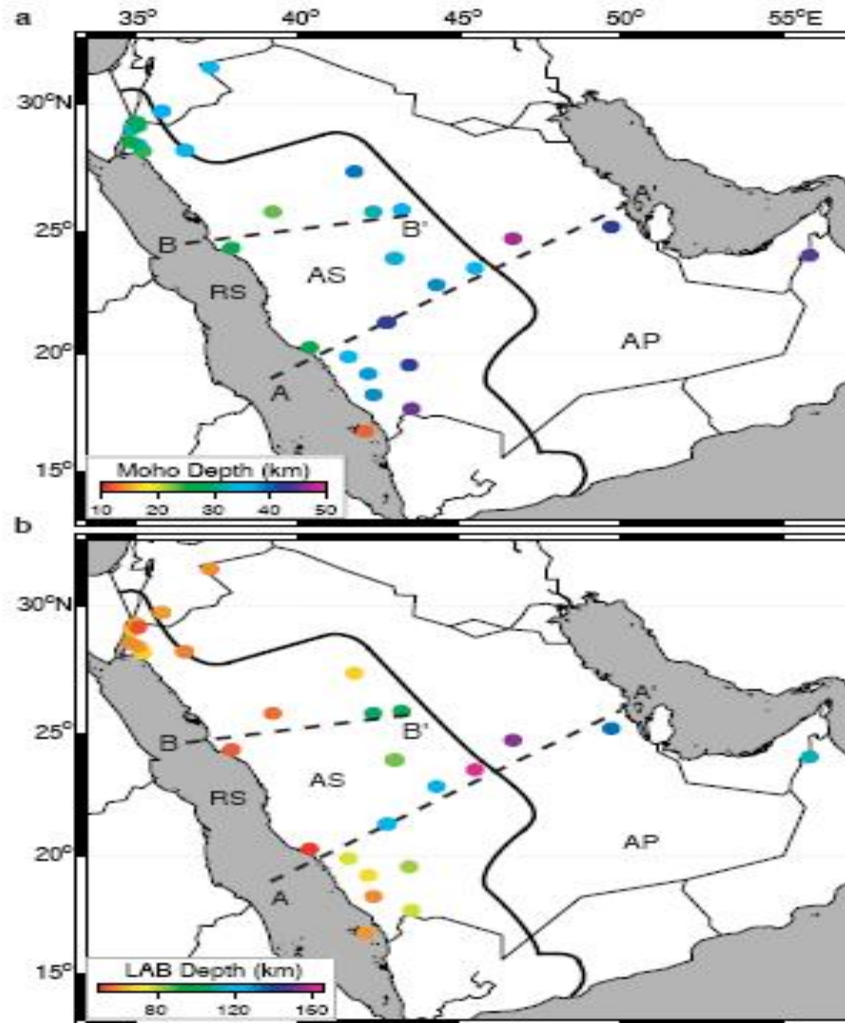


Figure 5.33. Maps showing the boundary depths beneath Arabia. The colored circles show the **a)** Moho and **b)** LAB depths beneath individual stations where warmer colors indicate shallower depths than cooler colors. The solid line marks the boundary between the Arabian Shield (AS) and the Arabian Platform (AP) while the two dashed lines mark the locations of cross-sectional profiles AA' and BB'. Shallow (40-60 km) LAB along Red Sea coast and Gulf of Aqabah Thickens (80-120 km) toward interior of Shield Step (20-40 km) across the Shield-Platform boundary (Hansen et al., 2007).

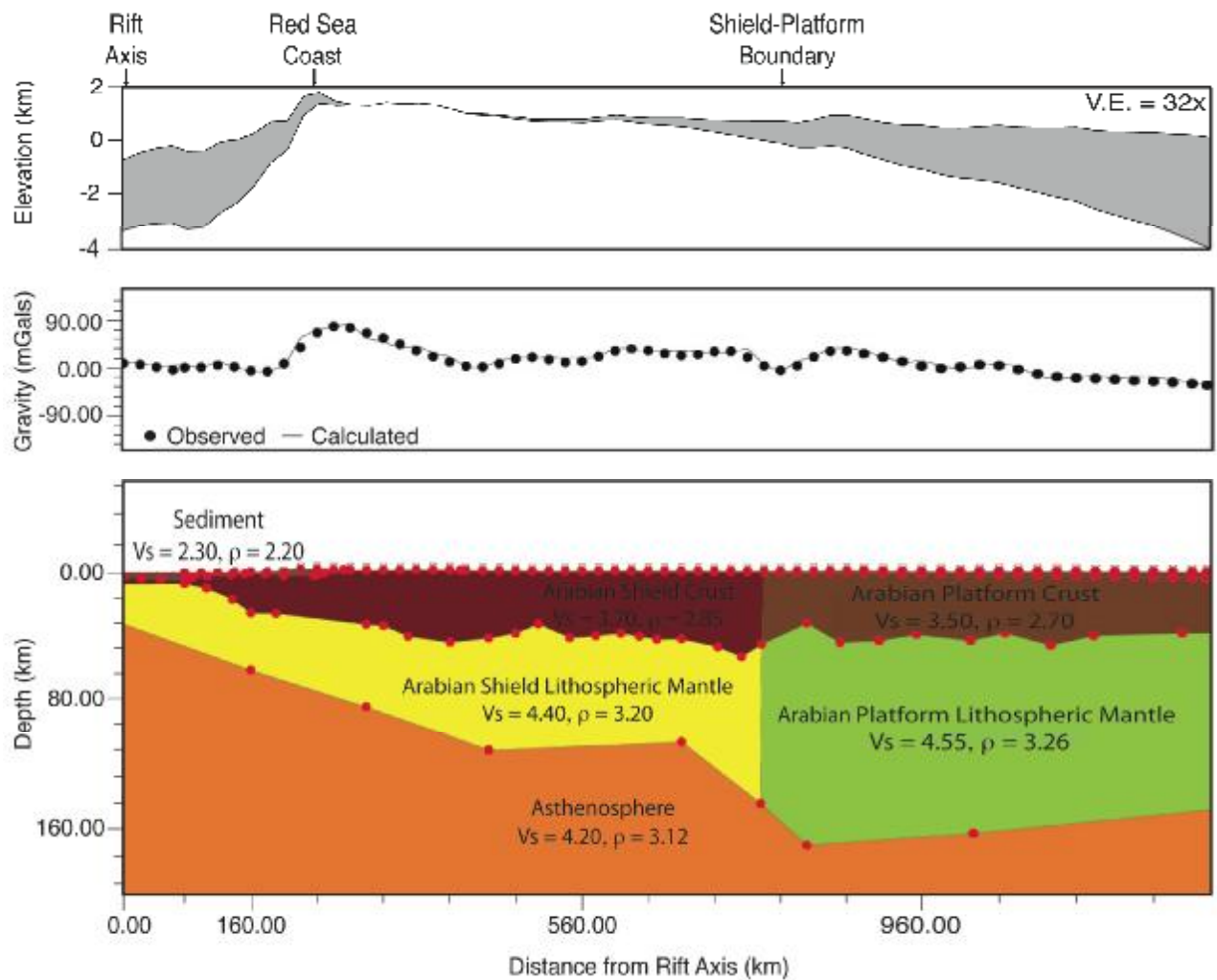


Figure 5.34. Topography, gravity signature, and lithospheric structure along cross-sectional profile AA' from Figure 5. **a** Topography along the profile plotted with a 32x vertical exaggeration (V.E.). The sediment thickness is shown by the grey shaded areas. **b** Comparison of the observed gravity data from the GRACE satellites (black dots) and the calculated gravity (grey line) resulting from the structural model shown in **c**. The S-wave velocities ( $V_s$ ) in km/s and densities ( $\rho$ ) in  $\text{g/cm}^3$  of each layer are listed (Hansen et al., 2007).

## Recent Crustal Structures

Al-Amri et al. (2004) performed the grid search using travel time data sets: (a) Pn and Pg; and (b) Pn, Pg and Sg. In order to select a single velocity model to be representative of the paths sampled, they made use of the results of a seismic refraction (*Ginzburg et al.*, 1979 ; El-Isa, 1990 and *Seber et al.*, 1997. Their grid search results with the thicker crusts (28-30 km) are consistent with these earlier studies. The preferred model has a crustal thickness of 28 km for the Gulf of Aqabah

**Table 6.1 Velocity Model for the Gulf of Aqabah/Dead Sea Region**

DEPTH (KM)	THICKNESS(KM)	V <sub>P</sub> (KM/S)	V <sub>S</sub> (KM/S)
0	2	4.50	2.60
2	5	5.50	3.18
7	10	6.10	3.52
17	11	6.20	3.60
28	∞	7.80	4.37

V<sub>P</sub> and V<sub>S</sub> are the P- and S-wave velocities, respectively.

Earlier work with waveform data from the 1995-1997 Saudi Arabian Broadband Deployment by the University of California, San Diego (UCSD) and King Saud University resulted in models for the Arabian Platform and Arabian Shield (*Rodgers et al.*, 1999). In that studied Love and Rayleigh wave group velocities were modeled to estimate average one-dimensional seismic velocity models of the two main geologic/tectonic provinces of Saudi Arabia. A grid search was used to quickly find a range of models that satisfactorily fit the dispersion data, then that range of models was explored to fit the three-component broadband (10-100 seconds) waveforms. The resulting models revealed significant differences between the lithospheric structure of the two regions.

**Table 6.2 Velocity Model for the Arabian Shield Region**

<b>DEPTH (KM)</b>	<b>THICKNESS(KM)</b>	<b>V<sub>P</sub> (KM/S)</b>	<b>V<sub>S</sub> (KM/S)</b>
0	1	4.0	2.31
1	15	6.20	3.58
16	20	6.80	3.93
36	∞	7.90	4.30

**Table 6.3 Velocity Model for the Arabian Platform Region**

<b>DEPTH (KM)</b>	<b>THICKNESS(KM)</b>	<b>V<sub>P</sub> (KM/S)</b>	<b>V<sub>S</sub> (KM/S)</b>
0	4	4.00	2.31
4	16	6.20	3.64
20	20	6.4	3.70
40	∞	8.10	4.55

To check the validity of the Arabian Platform, we measured Rayleigh and Love wave group velocities for a number of regional events from the Zagros Mountains and Turkish-Iranian Plateau. Paths from these events to the SANDSN stations sample the Arabian Platform.

Generally, we would suggest that low velocity beneath the Gulf of Aqabah and southern Arabian Shield and Red Sea at depths below 200 km are related to mantle upwelling and seafloor spreading. Low velocities beneath the northern Arabian Shield below 200 km may be related to volcanism. The low velocity feature near the eastern edge of the Arabian Shield and western edge of the Arabian Platform could be related to mantle flow effects near the interface of lithosphere of different thickness.

The results for crustal structure are consistent with previous studies where applicable. New results for the lithosphere suggest that the mantle lithosphere is thin and the LVZ is significant near the Red Sea, where rifting is active. The mantle lid thickens away from the Red Sea in the Arabian interior. Furthermore our results indicate the presence of polarization anisotropy in the lithospheric upper mantle, in the vicinity, as well as farther away from the Red Sea. Our modeling suggests  $v_{SV} > v_{SH}$  in the southern part of the Red Sea, consistent with vertical flow, and  $v_{SH} > v_{SV}$  in the northern part of the Red Sea and the continental interior, as is commonly reported in the continents. The Moho appears to be gradational, but the crustal thickness does not exceed 40 km, which is consistent with  $v_p/v_s$  analysis and inconsistent with a grid search analysis for receiver functions fits only. The mantle velocities are consistent with stable continental values.

Teleseismic shear-wave splitting along the Red Sea and across Saudi Arabia reveals that stations in the Gulf of Aqabah display fast orientations that are aligned parallel to the Dead Sea Transform Fault. However, our observations across Saudi Arabia show a consistent pattern of north-south oriented fast directions with delay times averaging about 1.4 s. While fossilized anisotropy related to the Proterozoic assembly of the Arabian Shield may contribute to our observations, we feel that the anisotropic signature is best explained by a combination of plate and density driven flow in the asthenosphere. Shear caused by the absolute plate motion, which is directed approximately 40° east of north at about 22 mm/yr, may affect the alignment of mantle minerals. Combining the northeast oriented flow associated with absolute plate motion with the northwest oriented flow associated with the mantle plume beneath Afar generates a north-south oriented resultant that matches our splitting observations.

## **RECOMMENDATIONS FOR FURTHER INVESTIGATIONS**

In order to fully understand the detail geophysical, seismological and seismic hazard picture of the Arabian Peninsula, this study recommends an extensive research covering :

- A. An expensive but potentially insightful line of research is to carry out a detailed seismic deep refraction and gravity profiles in the Arabian Platform and along the coast of the Gulf of Aqabah to obtain a precise bulk composition of crustal layers and improve velocity model.
- B. Upgrading of the existing system at King Saud University from analog to digital broadband recordings is strongly recommended for getting better quality signals.
- C. Linking of KACST and KSU seismic networks with the national seismographic network at the Saudi Geological Survey is of great importance for getting better and dense station coverage as well as in facilitating data exchanges.
- D. Installation of strong motion accelerographs in various areas of the Arabian Shield to precisely estimate the attenuation characteristics of the region and to improve seismic hazard parameters.
- E. Assessment of seismic hazard in seismically active zones by constructing a probabilistic ground-shaking hazard map. This map will provide an estimate of the level of ground shaking at all sites expected from earthquake sources throughout the region (both local and regional). The map integrates the seismicity, attenuation and sit response factors.
- F. A comprehensive study of the geotechnical engineering aspects should be done to account for local site effects and soil amplification.
- G. A comprehensive study of seismogenic and faulting sources is needed for seismic zonation and microzonation of the Arabian Penninsula.